11-17-2011

Copper Layers Deposited on Aluminum by Galvanic Displacement

Jiahe Ai
Iowa State University

S. P. Liu
Iowa State University

Newira A. Widharta
Iowa State University, newirawidharta@gmail.com

See next page for additional authors

THE JOURNAL OF PHYSICAL CHEMISTRY C

ARTICLE

pubs.acs.org/JPCC

Copper Layers Deposited on Aluminum by Galvanic Displacement

J. H. Ai,[†,§] S. P. Liu,[†] N. A. Widharta,[†] S. Adhikari,[†] J. W. Anderegg,[‡] and K. R. Hebert*[,†]

[†]Department of Chemical and Biological Engineering, Iowa State University, Ames, Iowa 50011, United States

[‡]US DOE, Ames Laboratory, Ames, Iowa 50011, United States

ABSTRACT: Metallization layers nanometers to tens of nanometers thick are desirable for semiconductor interconnects, among other technologically relevant nanostructures. Whereas aqueous deposition of such films is economically attractive, fabrication of continuous layers is particularly challenging on oxidized substrates used in many applications. Here it is demonstrated that galvanic displacement can deposit thin adherent copper layers on aluminum foils and thin films from alkaline copper sulfate baths. According to scanning electron microscopy and quartz crystal microbalance measurements, the use of relatively low $CuSO_4$ concentrations produced films composed of copper nanoparticles overlying a uniform continuous copper layer on the order of nanometers in thickness. It seems that there are no precedents for such thin layers formed by aqueous deposition on oxidized metals. The thin copper layers are explained by a mechanism in which copper ions are reduced by surface aluminum hydride on Al during alkaline dissolution.

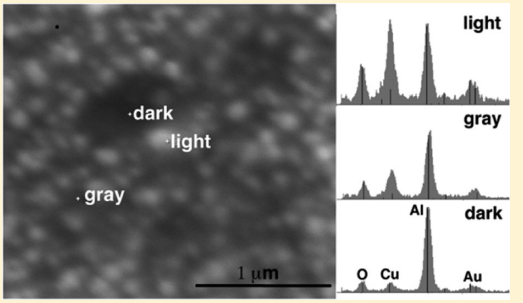

INTRODUCTION

Because of their cost effectiveness, solution-based thin-film deposition techniques are widely integrated in semiconductor interconnect and MEMS technology. "Ultrathin" metallization layers of a few nanometers thickness are particularly beneficial in applications involving nanostructured substrates. In semiconductor interconnects, the ability to produce such deposits would eliminate the need for vapor-deposited seed layers for copper electrodeposition on TaN or TiN barrier materials. Efforts to produce seed layers by direct electrodeposition onto the barrier are hindered by the insulating, spontaneously formed oxide films on these materials.[1−4] Electroless deposition (ELD) methods, in which the deposited metal ion is chemically rather than electrochemically reduced, are attractive because they do not require conductive substrates. ELD of Cu on barrier materials has been demonstrated.[5−7] Galvanic displacement, in which either the substrate itself or adsorbed atoms reduce the deposited metal ions, has been explored extensively for fabrication of metal films on semiconductors and noble metals,[8,9] and copper layers on barrier materials have been reported.[10,11] However, it seems that ultrathin films on oxidized substrates have not yet been fabricated by either ELD or galvanic displacement.

The present Article concerns the deposition of thin copper layers on aluminum by galvanic displacement. Aluminum exemplifies substrates having a surface oxide that interferes with solution-phase thin film deposition. Micron-thick particulate Cu films displaying good adhesion can be electrodeposited from alkaline sulfate baths;[12] also, several techniques have been developed to disrupt Al oxide layers to promote electrodeposition.[13−16] Evidence of these papers suggests that deposition is promoted by alkaline solutions or by cathodic applied potentials at which hydrogen evolution generates alkalinity near the Al surface. Galvanic displacement methods have been used to deposit copper and nickel films on Al from NaOH solutions,[17,18] silver particles on aluminum−copper alloy films from nitrate solution,[19] and silver dendrites on Al from fluoride solution.[20]

The mechanism of galvanic displacement in alkaline solutions may involve surface hydride species. Whereas the portion of the surface film on Al contacting the alkaline solution is composed of aluminum oxide or hydroxide,[21] evidence from our laboratory supports previous findings by Perrault that the interior of the film contains appreciable (AlH_3).[22] We detected interfacial aluminum hydride within the surface film by secondary ion mass spectrometry and atom probe tomography (APT)[23,24] and showed that the electrochemical potential at the metal−film interface is close to the Nernst potential of the hydride oxidation reaction.[25,26] Because borohydride ions in solution can mediate ELD of copper from alkaline baths, a similar role for surface AlH_3 seems possible[27,28]

We show here that simple galvanic displacement from alkaline baths can deposit thin Cu metal layers on Al in certain ranges of pH, copper concentration, and process time. Low copper concentrations seem to favor thin layer deposits, whereas particulate deposits are found at higher concentrations. The kinetics of deposition in its initial stages on Al foils and thin films were followed using quartz crystal microbalance (QCM) and open circuit potential measurements. From QCM and scanning electron microscopy (SEM) results, we estimate that the thin layers are on the order of nanometers in thickness. The present results provide complementary evidence of the nanometer-thick copper films found in an APT analysis of Cu deposits on high-curvature Al surfaces.[24] We know of no precedent for the formation of such

Received: June 9, 2011
Revised: September 5, 2011
Published: October 05, 2011

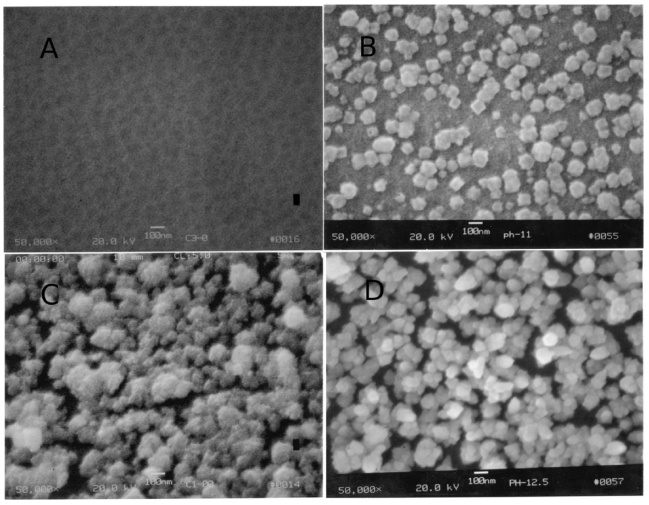

Figure 1. Secondary electron images after 25 s of Cu open-circuit deposition in 50 mM $CuSO_4$ with 10 mM Na_2SO_4 and 100 mM EDTA at (A) pH 10; (B) pH 11, (C) pH 11.75, and (D) pH 12.5.

ultrathin metallization layers on oxidized substrates by aqueous deposition methods.

EXPERIMENTAL SECTION

The substrates for copper deposition were 99.99% purity Al foils or thin films. The foil thickness was 127 μm and its typical grain size was 100 μm (Toyo). Prior to deposition, the foils were electropolished at 5 °C and 30 V for 5 min, in a solution of 20% perchloric acid (70%) and 80% ethanol (98%). Electropolishing removed an impurity- enriched surface region that is produced by the rolling step in the processing of Al foils. Deposition onto foils was conducted in a glass cell, in which the exposed area of the upward-facing Al surface was 0.637 cm^2. Potential sweep experiments were carried out in the same cell with a potentiostat (CH Instruments), Pt wire counter electrode, and Ag/AgCl (saturated KCl) reference electrode. All cited potential values are expressed relative to this reference. Thin film samples were used for in situ measurements of the copper deposition rate by the QCM technique. AT-cut quartz crystals were employed with 200 nm thick evaporated Al films and resonant frequency 7.995 MHz (International Crystal Manufacturing). The glass cell of a commercial QCM was used for these measurements (CH Instruments). The mass change was calculated from the measured frequency shift according to the Sauerbrey equation.[29]

In each deposition experiment, the Al substrate was first immersed at open circuit for a specified time in 5 mL of 0.1 M Na_2SO_4 solution. Alkaline exposure reduced the oxide thickness. The pH was adjusted to values between 10 and 13 by addition of NaOH crystals and small amounts of H_2SO_4 solution. Open circuit copper deposition was initiated by the addition of 45 mL of $CuSO_4$ containing solution at the same pH. After mixing, the deposition bath contained 10 mM Na_2SO_4, 100 mM EDTA, and specified concentrations of $CuSO_4$ between 1 and 100 mM. EDTA refers to the sodium salt of ethylenediamine tetraacetic acid, a strong complexing agent used to solubilize cupric ions in alkaline plating solutions. The quantity of copper deposit was determined by anodic stripping voltammetry, after replacing the deposition bath with pH 2 Na_2SO_4 solution. In this acidic solution, Al corrosion was suppressed in the potential range of Cu oxidation. All deposition and voltammetry experiments were performed at 21 °C, using reagent grade chemicals and nanopure water.

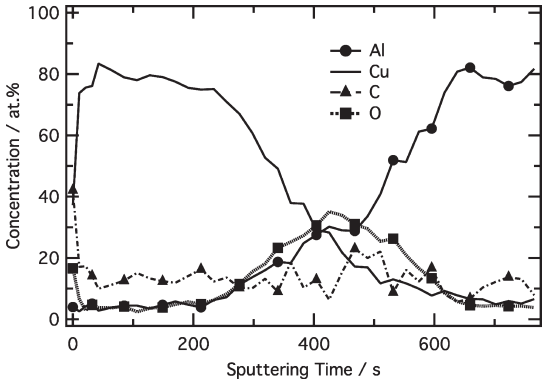

Figure 2. Scanning Auger microprobe composition analysis of Al sample after 2 min deposition in 50 mM $CuSO_4$ with 10 mM Na_2SO_4 and 100 mM EDTA at pH 11.75.

The morphology and composition of the deposited copper films were examined with the SEM and scanning Auger microprobe (SAM). The SEM instruments used in Figures 1 and 4 (Amray 1845 and FEI Quanta 250, respectively) were equipped with field-emission guns and energy-dispersive spectrometers (EDS). The SAM employed a field-emission SAM (JEOL JAMP-7830F) with a lateral resolution of ~200 nm. The electron beam voltage and current for Auger were 15 kV and 10 nA, and the sample stage was tilted to 30°. The measured count intensity of detected Cu, Al, O, and C signals was converted to atomic percent using the sensitivity factors from JEOL software. Additionally, characterizations of the adhesion of copper films were carried out, following the ASTM tape test.[30]

RESULTS AND DISCUSSION

Characterization of Deposits. In 50 mM $CuSO_4$ solutions, copper particles nucleated rapidly above a critical pH. Figure 1 shows SEM images after 25 s of deposition at pH values from 10 to 12.5. No deposited particles were detected at pH 10, but increasing numbers of ~100 nm diameter particles formed at higher pH values. The particle number density was $>10^{10}$ cm^{-2} at pH 11.75 and 12.5. The Cu EDS peak increased with pH with the same trend as the particle number density; for example, the copper peak intensity at pH 10 was ~100 times smaller than that at pH 11.75. EDS further showed that the particles were enriched in copper but not oxygen relative to the surrounding surface, indicating that they were likely copper metal as opposed to a precipitated hydroxide phase. Therefore, the EDS results supported the identification of the particles as copper metal. After 2 min of deposition at pH 11.75 or higher, SEM images (not shown) indicated that particles had continued to nucleate, forming a dense surface layer. The minimum pH of 11 to 12 for deposition corresponds to the limiting pH, above which the surface oxide on Al is soluble.[31]

SAM measurements were used to analyze the deposit formed in 50 mM $CuSO_4$ at greater depth and lateral spatial resolution than was possible with EDS. Figure 2 shows a SAM depth profile at a selected area ~200 nm in diameter, after deposition for 2 min at pH 11.75. SEM showed that the particle density was higher than in Figure 1c and that the mean particle diameter was

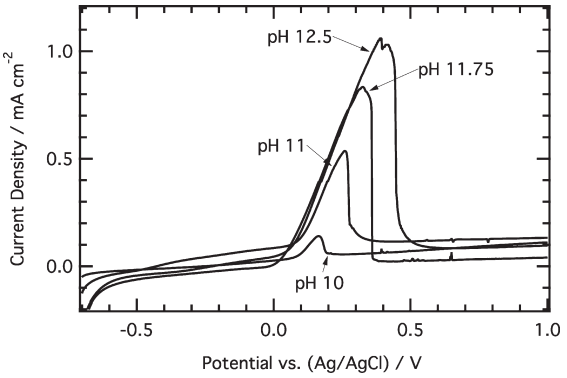

Figure 3. Anodic stripping voltammetry in pH 2 Na_2SO_4 solution after 25 s of Cu open-circuit deposition in 50 mM $CuSO_4$ with 10 mM Na_2SO_4 and 100 mM EDTA at pH 10, 11, 11.75, and 12.5. Scanning rate is 5 mV/s.

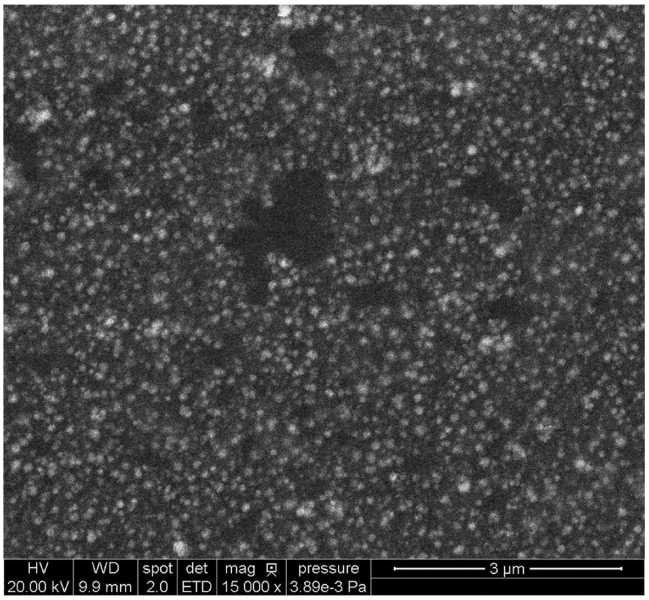

Figure 4. Secondary electron image for an Al thin film substrate after deposition in 5 mM $CuSO_4$ with 10 mM Na_2SO_4 and 100 mM EDTA at pH 11.75. Deposition was initiated by $CuSO_4$ addition after 10 s of alkaline immersion and continued for a period of 105 s.

~100 nm; hence, the SAM profile includes oxidized Al surface between copper particles. The depth profile in Figure 2 was typical of those obtained at several locations on the sample. The profile reveals an outer copper layer with 12−16 at % carbon and ~5 at % oxygen and aluminum. The carbon likely results from gas-phase contaminants adsorbed on the lateral surfaces of Cu particles; on a carbon-free basis, the outer layer contained 88 at % Cu and 6 at % O and Al. The correlation of Al and O profiles in Figure 2 suggests that the latter signals are due to either the oxidized Al substrate or precipitated $Al(OH)_3$ between the particles. The high Cu fraction in the deposit layer confirms that particles contained metal rather than copper oxides.

Additional analysis of deposits from 50 mM $CuSO_4$ solution was carried out using anodic stripping voltammetry (ASV), which samples the entire metal surface, unlike EDS and SAM. For ASV, the samples were transferred from the deposition bath into an electrochemical cell containing a pH 2.0 Na_2SO_4 solution. The use of an acidic solution for ASV avoided contributions to the measured anodic current from Al corrosion. The current−potential scans after 25 s of deposition, shown in Figure 3, display the expected anodic Cu dissolution peak above 0.0 V, with no other voltammetric features.[2] Like the particle number density in Figure 1, the anodic charge encompassed by the peak increases with deposition pH. Only a small charge was detected after deposition at pH 10, at which SEM revealed no copper particles. The anodic stripping charge at pH 10, 11, and 11.75 was 1.6, 8.7, and 32 mC/cm^2, respectively, equivalent to uniform copper layer thicknesses of 0.59, 3.2, and 12 nm. The latter values would agree with the particle coverages suggested by Figure 1, if the particles are tens of nanometers in height. In combination, the EDS, SAM, and ASV results demonstrate that copper metal deposits at a high rate at open circuit.

Table 1. Percent Adhesion of Copper Films Deposited from 50 mM $CuSO_4$ Solutions

deposition time	pH 11.74	pH 12.25	pH 13.0	pH 13.5
25 s	90%	50%	10%	90%
2 min	100%	100%	95%	90%

Deposits on reactive metals such as Al are often poorly adherent because of high roughness resulting from low nucleation rates on the surface oxide. Results of the ASTM standard tape test of adhesion are listed in Table 1 for copper films formed from 50 mM $CuSO_4$ solutions. The films deposited at pH values of 12.5 or lower for 2 min were highly adhesive, whereas adhesion was relatively poor after 25 s of deposition in the same baths.[30] In this pH range, adhesion correlated with the continuity of the film as revealed by SEM. However, the films deposited at pH 13.0, while continuous, were also very rough and adhered poorly, probably due to rapid corrosion at high pH. In general, adherent films were obtained when the deposition conditions promoted high surface coverage and minimized substrate corrosion.

Evidence of Cu thin layers between the particles was found after deposition from 5 mM $CuSO_4$ solutions. Figure 4 shows an FE-SEM secondary electron image of an Al thin film sample after 10 s of immersion at pH 11.75, followed by 105 s copper deposition. A gray film with interspersed particles covers the substrate; the exposed Al metal at holes in the film has distinctly darker contrast. Figure 5 displays a higher magnification secondary electron image of the same sample, in which a relatively high beam current was selected to increase X-ray emission, and a beam voltage of 5 kV was used at which the lateral resolution of EDS is on the order of 100 nm. The local X-ray spectra on the right of the Figure indicate that the areas with "light," "gray", and "dark" atomic number contrast correspond to decreasing ratios of Cu to Al concentration. The light regions are copper particles, with similar dimensions but smaller number density compared with those in Figure 1. The dark areas are the same isolated copper-free patches in Figure 4, whereas the areas with gray contrast that cover much of the surface between particles contain significantly more copper than the dark regions. The absence of morphological features in the gray area suggests that a uniform thin film containing either copper metal or copper oxide occupied this region.

The thickness of the thin copper-containing layer between particles may be estimated using the mass change of 3.4 μg/cm^2 measured in this experiment by QCM. Assuming that 1.5 Cu atoms deposit for each dissolved Al atom, this mass change is

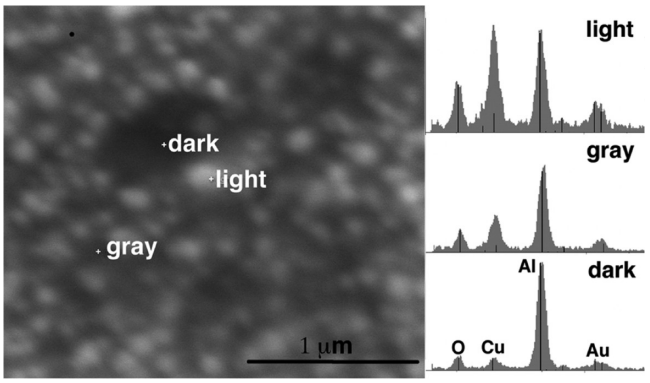

Figure 5. High magnification secondary electron image of the sample in Figure 4 with local EDS demonstrating the composition of regions with dark, gray, and light contrast.

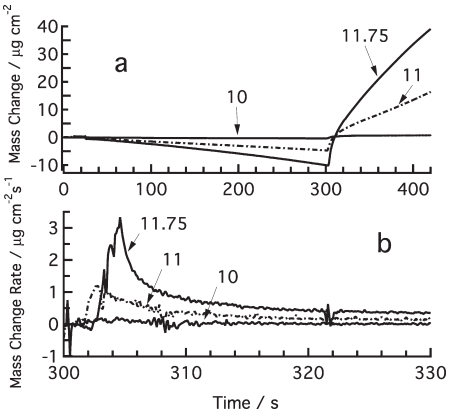

Figure 6. (a) QCM mass transients during open-circuit deposition at pH 10, 11, and 11.75. $CuSO_4$ solution was added at 300 s. The solution composition during copper deposition was 50 mM $CuSO_4$ with 10 mM Na_2SO_4 and 100 mM EDTA. (b) Time derivative of the mass change during copper deposition.

equivalent to an average Cu layer thickness of ~5.4 nm. Also, the EDS in Figure 5 suggests that the particles contain roughly four times more Cu than the thin layer, and according to the SEM image, they occupy about half of the sample area. Accordingly, the order of magnitude estimate of the Cu layer thickness between the particles is 2 nm. The continuous copper film detected by APT on needle-shaped samples was 1 nm thick.[24] To our knowledge, such ultrathin deposits have not been previously reported in studies of aqueous deposition on oxidized metals, as deposition is typically confined to isolated defects in the oxide.

In summary, the characterization studies showed that copper deposited on aluminum at a high rate, above a minimum pH of 11 to 12 corresponding to the limit of oxide stability. The deposits contained large numbers of roughly 100 nm Cu particles. Evidence of an underlying Cu thin film was also found at low $CuSO_4$ concentration. The next section describes additional studies using the QCM and open-circuit potential measurements to determine the factors controlling the deposit morphology and deposition rate.

Kinetics of Deposition. QCM measurements revealed the transient progress of deposition onto Al thin films. Figure 6a

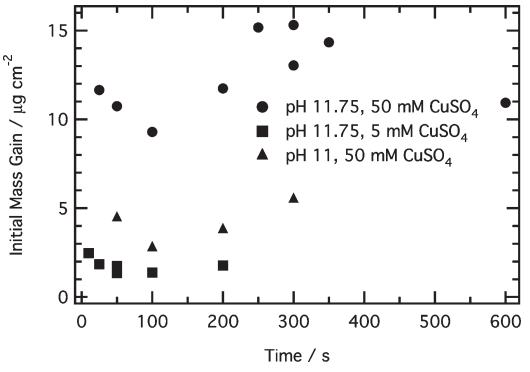

Figure 7. Mass gain measured with QCM during the first 12 s after adding $CuSO_4$ for various addition times and bath compositions.

shows mass transients in experiments at pH 10, 11, and 11.75, in which 50 mM $CuSO_4$ solution was added after 300 s of open circuit immersion. Before copper addition, the mass decreased because of Al corrosion. The average corrosion rate increased with pH, as expected due to the effect of alkalinity on the solubility of the surface oxide film. The corrosion rate at pH 11.75, 13 mg/dm^2 h, agrees with a literature value of 10 mg/dm^2 h at pH 12.[31] The mass increased abruptly when copper solution was introduced at 300 s. The rate of mass change during deposition, determined by numerical differentiation of the QCM mass transients, is shown in Figure 6b. After an initial delay due to mixing of the added solution, the mass increased rapidly for 5−10 s and subsequently at a much smaller rate. If the mass increase from 300 to 325 s was primarily due to copper deposition, the equivalent stripping charges at pH 10, 11, and 11.75 would be 2.8, 26, and 58 mC/cm^2. The increasing trend with pH is the same as that from ASV of foils, but at each pH, the equivalent charges from QCM are 2 to 3 times larger than the ASV charges. This discrepancy is possibly due to incomplete stripping or higher deposition rates on film than foil samples. Figure 7 compiles the mass gain during the first 12 s after $CuSO_4$ addition, that is, the period of rapid mass increase exhibited by Figure 6b, for experiments with various deposition times, pH values, and copper concentrations. The initial mass change increased strongly with bath copper concentration and pH, the same as the trends of the particle number density indicated by SEM. Interestingly, the initial mass changes of 1 to 2 μg/cm^2 measured in 5 mM $CuSO_4$ are equivalent to copper layer thicknesses on the order of 1 nm, similar to that of the thin Cu layer in Figures 4 and 5.

Open circuit potential transients on Al foils also exhibited features suggesting a distinct initial stage of deposition. Figure 8a, b illustrates the effects of pH and copper concentration, respectively, on the potential transient during deposition. In Figure 8a, the initial potentials prior to deposition correspond to the Nernst potential of the equilibrium of AlH_3 with aluminum oxide.[22,26] The addition of copper ions caused the potential to increase rapidly, after which clear maxima or plateaus were observed, followed by slow drift in the anodic direction. As the pH increased, the time elapsed during the initial maxima decreased, from ~25 s at pH 11.75 to 10 s at pH 12.5. The time of the initial peak at pH 11.75 corresponds to the period of rapid mass change in the QCM transient (Figure 6b).

The measured open-circuit potentials were compared with potentials during electrodeposition from the same Cu^{2+}-EDTA

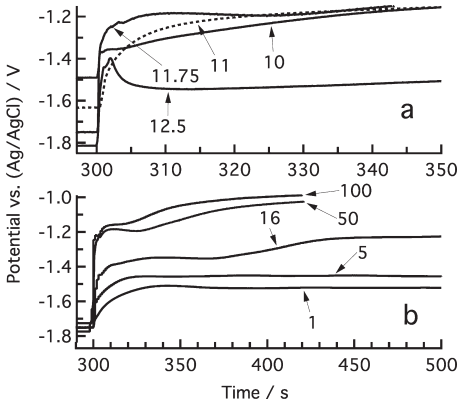

Figure 8. Open circuit potential transients of copper deposition experiments. (a) Effect of pH at 50 mM $CuSO_4$. After immersion of Al samples for 300 s in 10 mM M Na_2SO_4, copper-containing solutions were added to achieve the final composition 50 mM $CuSO_4$ with 10 mM Na_2SO_4, and 0.1 M EDTA. (b) Effect of $CuSO_4$ concentration at pH 11.75. Immersion for 300 s in 10 mM Na_2SO_4 at pH 11.75 was followed by copper addition to obtain baths with the indicated $CuSO_4$ concentrations in 10 mM Na_2SO_4 and 0.1 M EDTA at pH 11.75.

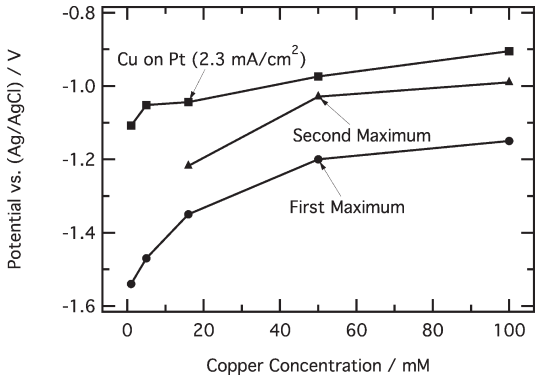

Figure 9. Maximum potentials of open circuit potential transients versus copper concentration (i.e., Figure 3b) in baths containing 10 mM Na_2SO_4 and 0.1 M EDTA at pH 11.75. The square symbols are potentials of Pt electrodes in the same solutions measured during copper electrodeposition, in which the Pt potential was scanned in the anodic direction at 5 mV/s from −1.5 V; the potential at the cathodic current density of 2.3 mA/cm^2 is displayed.

baths. Figure 9 shows the potential of the initial maximum for deposition at pH 11.75 and that of the final plateau or "second maximum." Also shown is the potential during electrodeposition onto Pt wires from the same $CuSO_4$/EDTA solutions at a cathodic current density of 2.3 mA/cm^2, equivalent to a representative rate of mass increase during open circuit deposition. The potential values were recorded after the Pt wires had been coated with electrodeposited copper and therefore correspond to electrodeposition onto a Cu substrate. Note that strong complexation of Cu^{2+} ions by EDTA shifts the deposition potential by several hundred millivolts in the cathodic direction.[2] Figure 9 shows that the potential of the second maximum was within ~100 mV of the electrodeposition potential. This close proximity suggests that open-circuit deposition occurred mainly by direct plating onto Cu particles, which cover the Al surface at the time of the second maximum (Figure 1). As previously found by Djokic, anodic aluminum dissolution supported the deposition reaction as well as cathodic hydrogen evolution on the particles.[17] The distinctly more negative deposition potentials during the initial maxima suggest that different reaction kinetics apply at these times. In the initial stage of deposition, the potential may be influenced by the reactions forming the thin copper layer in Figures 4 and 5; as noted above, for 5 mM $CuSO_4$ solution, the mass increase during the initial maxima agrees with the estimated copper layer thickness.

Galvanic Displacement Mechanism. Evidence of nanometer thick copper films was also found by atom probe topography (APT) on the tips of needle-shaped Al wires after deposition from 50 mM $CuSO_4$ solution.[24] Comparison with samples exposed to copper-free alkaline baths showed that Cu deposition was accompanied by loss of surface oxide; about one O atom was seemingly removed per Cu atom deposited. The apparent exchange of Cu and O is evidence that the galvanic displacement reaction involves a surface hydride layer on Al during alkaline etching.[22,23,25,26] In the presence of Cu^{2+} ions, surface AlH_3 reacts to form Cu metal; on the other hand, upon emersion from copper-free solutions, most of the hydride reacts with water or oxygen to form oxide. The continuity of the ultrathin Cu deposit can be explained by the high coverage of this hydride layer. The deposition mechanism is probably similar to that of electroless Cu deposition in alkaline baths containing $NaBH_4$ reducing agent,[27,28] except that Al metal as well as surface hydride can reduce copper ions.

The thickness and coverage of the thin copper layer in Figures 4 and 5 are similar to those of the APT-detected films and thus show that the hydride-mediated deposition process is not limited to high-curvature substrates. The hydride mechanism also seems to reconcile the initial mass change from QCM with the apparent thickness of the Cu layer found in SEM. For 5 mM $CuSO_4$ baths, the SEM images show that thin Cu layers contribute appreciably to the overall deposited mass, and so a significant portion of the initial mass change of 1 to 2 μg/cm^2 in Figure 7 should be due to the thin layer. According to the hydride mechanism, the mass change per mole of Cu deposited is 44 g/mol, from which this mass change corresponds to Cu layer thicknesses of 1.6 to 3.2 nm. A comparable Cu layer thickness of 1 nm was estimated from the SEM and EDS results in Figure 4, as discussed above. Also, a Cu layer thickness of 1 nm implies preexisting AlH_3 surface concentrations of $(5 \text{ to } 9) \times 10^{-9}$ mol/cm^2, depending on the contribution of Al as a reducing agent. This range is on the same order of magnitude as the concentration of residual AlH_x^+ ions of 2×10^{-9} mol/cm^2 detected by APT after exposure of Al to copper-free solutions. The lower measured concentration is likely due to air oxidation of hydride after emersion of the sample.

These comparisons support the view that the initial rapid deposition process involves copper reduction by a surface AlH_3 layer, producing an ultrathin Cu film. At later times, copper particles increasingly cover the surface, and deposition occurs by particle growth accompanied by Al corrosion. Efforts to promote layer over particle growth should focus on the deposition experiments using relatively small copper concentrations and limited to small exposure times.

CONCLUSIONS

In this Article, we reported the use of galvanic displacement to deposit thin copper films on aluminum from alkaline $CuSO_4$−EDTA

solutions. Adherent films containing high number densities of Cu particles were formed from 50 mM $CuSO_4$ baths at pH 11.75 to 12.5. When 5 mM $CuSO_4$ solutions were used, SEM examination revealed copper layers on the order 1 nm thickness, similar to deposits on the tips of thin Al wires, which were characterized by APT.[24] The present results show that formation of ultrathin films does not require the use of high-curvature substrates and that film formation is promoted by small bath copper concentrations and limited deposition times. To our knowledge, this is the first evidence of such ultrathin films formed by aqueous deposition on oxidized metal substrates. Studies of deposition kinetics using QCM and open circuit potential measurements suggested a distinct initial stage of rapid deposition, which seems to account for the mass change associated with the thin copper layer. We suggest that the thin layer is templated by interfacial AlH_3 present on Al during alkaline corrosion. The results indicate new possibilities to prepare nanometer-thick metallization layers on oxidized metals. In particular, similar processes could occur on other hydride-forming metals, such as titanium, zirconium, and magnesium.

AUTHOR INFORMATION

Corresponding Author

*E-mail: krhebert@iastate.edu.

Present Addresses

[§]Department of Materials Science and Engineering, University of Virginia, Charlottesville, Virginia, United States.

ACKNOWLEDGMENT

This work was supported by the National Science Foundation through grant DMR-0605957. We thank Professor L. Scott Chumbley for his help in obtaining the SEM image in Figure 4.

REFERENCES

(1) Oskam, G.; Vereecken, P. M.; Searson, P. C. *J. Electrochem. Soc.* **1999**, *146*, 1436–1441.
(2) Radisic, A.; Cao, Y.; Taephaisitphongse, P.; West, A. C.; Searson, P. C. *J. Electrochem. Soc.* **2003**, *150*, C362–C367.
(3) Radisic, A.; Oskam, G.; Searson, P. C. *J. Electrochem. Soc.* **2004**, *151*, C369–C374.
(4) Kim, S.; Duquette, D. J. *J. Electrochem. Soc.* **2006**, *153*, C673–C676.
(5) Dubin, V. M.; Shacham-Diamand, Y.; Zhao, B.; Vasudev, P. K.; Ting, C. H. *J. Electrochem. Soc.* **1997**, *144*, 898–908.
(6) O'Kelly, J. P.; Mongey, K. F.; Gobil, Y.; Torres, J.; Kelly, P. V.; Crean, G. M. *Microelectron. Eng.* **2000**, *50*, 473–479.
(7) Kim, J. J.; Kim, S. K.; Lee, C. H.; Kim, Y. S. *J. Vac. Sci. Technol., B* **2003**, *21*, 33–38.
(8) Carraro, C.; Maboudian, R.; Magagnin, L. *Surf. Sci. Rep.* **2007**, *62*, 499–525.
(9) Thambidurai, C.; Kim, Y. G.; Jayaraju, N.; Venkatasamy, V.; Stickney, J. L. *J. Electrochem. Soc.* **2009**, *156*, D261–D268.
(10) Wu, Y.; Chen, W. C.; Fong, H. P.; Wan, C. C.; Wang, Y. Y. *J. Electrochem. Soc.* **2002**, *149*, G309–G317.
(11) Wang, Z. C.; Li, H. Q.; Shodiev, H.; Suni, I. I. *Electrochem. Solid-State Lett.* **2004**, *7*, C67–C69.
(12) Bettelheim, A.; Raveh, A.; Mor, U.; Ydgar, R.; Segal, B. *J. Electrochem. Soc.* **1990**, *137*, 3151–3153.
(13) Rabin, O.; Herz, P. R.; Lin, Y. M.; Akinwande, A. I.; Cronin, S. B.; Dresselhaus, M. S. *Adv. Funct. Mater.* **2003**, *13*, 631–638.
(14) Choi, J.; Sauer, G.; Nielsch, K.; Wehrspohn, R. B.; Gosele, U. *Chem. Mater.* **2003**, *15*, 776–779.
(15) Tian, M. L.; Xu, S. Y.; Wang, J. G.; Kumar, N.; Wertz, E.; Li, Q.; Campbell, P. M.; Chan, M. H. W.; Mallouk, T. E. *Nano Lett.* **2005**, *5*, 697–703.
(16) Oh, J.; Thompson, C. V. *Adv. Mater.* **2008**, *20*, 1368–1372.
(17) Djokic, S. S. *J. Electrochem. Soc.* **1996**, *143*, 1300–5.
(18) Watanabe, H.; Honma, H. *J. Electrochem. Soc.* **1997**, *144*, 471–476.
(19) Brevnov, D. A.; Olson, T. S.; Lopez, G. P.; Atanassov, P. *J. Phys. Chem. B* **2004**, *108*, 17531–17536.
(20) Gutes, A.; Carraro, C.; Maboudian, R. *J. Am. Chem. Soc.* **2010**, *132*, 1476–+.
(21) Heusler, K. E.; Allgaier, W. *Werkst. Korros.* **1971**, *22*, 297–302.
(22) Perrault, G. G. *J. Electrochem. Soc.* **1979**, *126*, 199–204.
(23) Adhikari, S.; Lee, J. J.; Hebert, K. R. *J. Electrochem. Soc.* **2008**, *155*, C16–C21.
(24) Zhang, Y.; Ai, J. H.; Hillier, A. C.; Hebert, K. R. *Langmuir* **2011** submitted.
(25) Adhikari, S.; Hebert, K. R. *J. Electrochem. Soc.* **2008**, *155*, C189–C195.
(26) Adhikari, S.; Hebert, K. R. *Corros. Sci.* **2008**, *50*, 1414–1421.
(27) Lukes, R. M. *Plating* **1964**, *51*, 1066–8.
(28) Vaskelis, A.; Juskenas, R.; Jaciauskiene, J. *Electrochim. Acta* **1998**, *43*, 1061–1066.
(29) Buttry, D. A.; Ward, M. D. *Chem. Rev.* **1992**, *92*, 1355–1379.
(30) *Annual Book of ASTM Standards*; ASTM International: West Conshohocken, PA, 2008; Vol. 6.01, p 399.
(31) Pourbaix, M. *Atlas of Electrochemical Equilibria in Aqueous Solutions*; NACE International: Houston, 1974.